Wideband Metasurface Loaded Circularly Polarized MIMO Microstrip Antenna with High Isolation

Mukesh Tiwari, Kokab Afroz and Mehajabeen Fatima

Abstract – **In this article, dual port microstrip antenna with wideband characteristics is designed and developed. The attracting features of proposed antenna are: (a) loading of DGS reduce the Q-factor of antenna and improve the impedance bandwidth; (b) proposed metasurface acts as a LP (Linear Polarization) to CP (Circular Polarization) convertor and produces the circularly polarized waves within the operating band; and (c) same metasurface comes under the category of SNG and improves the isolation between the antenna ports by an amount of 15 dB. Experimental outcomes confirm the proposed antenna works from 12.2 GHz to 14.2 GHz. 3-dB axial ratios is achieved from 13.2 GHz to 13.9 GHz with left handed circular polarization feature. Good value of diversity parameter and far-field value confirms its suitability for Ku band applications.**

Keywords – **MIMO antenna, Metasurface, Wideband antenna, Circular polarization.**

I. Introduction

In the current wireless communication world, multi input and multi output (MIMO) radiators are widely used because of its ability to support higher data rate without any need of input power enhancement [1]. Microstrip radiator is one of the most suitable one for the designing of MIMO antenna because it has compact in size, conformal to planner and non-planner surfaces, easy to fabricate as well as integrate [2].

In literature, two major challenges have been faced by the researchers: high isolation between the ports and circular polarization features. For enhancing the isolation value, different techniques have been utilized such as Niu et al. proposed a H-shaped defected ground structure between the closely spaced patch antenna for getting the isolation more than 30 dB [3]. Li et al. placed a dielectric block over the dual port microstrip antenna for improving the isolation level by 20 dB.Dielectric block cancel the surface wave coupling between the antenna ports [4]. Hasan et al. loaded a metasurface for enhancing the isolation between the antenna ports by an amount of 15 dB [5]. In the similar manner, some of the researchers have given the techniques for circular polarization generation such as, Tiwari et al. proposed asymmetric Z-shaped radiator for creation the CP waves in between 4.42-6.11 GHz [6]. Malviya et al. proposed a 2*2 printed MIMO antenna. This radiator creates CP waves from 5.744ï 5.83 GHz by diagonally perturbing the microstrip radiator [7]. Ullah et al. proposed CPW fed monopole antenna, which supports the LHCP and RHCP waves separately by different antenna ports [8].

In this communication, a dual port microstrip antenna is designed for Ku band application. Metasurface is loaded above dual port microstrip antenna for enhancing the isolation around 15 dB as well as to create CP waves from 13.2 GHz to 13.9 GHz. Defected ground structure below the microstrip patch reduces the Q-factor, which in turn enhance the bandwidth of the radiator. The designed antenna works from 12.3 GHz to 14.2 GHz. For better understanding, the article is divided into different subsections: (i) geometrical layout of designed antenna; (ii) its analysis; (iii) experimental outcomes and diversity parameter; and (iv) final conclusion.

Article history: Received October 09, 2022; Accepted December 14, 2022

Mukesh Tiwari and Kokab Afroz are with the department of Electronics and Communication Engineering, Sri Satya Sai University of Technology & Medical Sciences, Sehore, Madhay Pradesh, India, E-mail: mukeshtiwari_79@yahoo.co.in, kokabafroz22@gmail.com

Mehajabeen Fatima is with department of Electronics and Communication Engineering, Sagar Institute of Research & Technology, Bhopal, Madhay Pradesh, India, E-mail: mehajabeen.fatima@gmail.com

II. Geometrical Layout of Designed Antenna

Structural layout and its fabricated structure are discussed in this section. Fig. 1 presents the schematic diagram of proposed antenna with its different view. Inset fed microstrip antenna has been etched over the FR-4 substrate ($\varepsilon_{sub} = 4.4$ and $\tan\delta = 0.02$). Defected ground structure (DGS) has been etched from the bottom surface of substrate. Fig. 1(c) shows the proposed LP to CP convertor, which is also fabricated over the FR4 substrate. It contains the periodic arrangement of rhombus shaped ring metallic structure. It is placed over the proposed dual port printed antenna. Table 1 lists the optimized dimension of different parameters of proposed antenna. Fig. 2 presents the pictures of fabricated antenna design, which is used for validation purpose.

TABLE 1
OPTIMIZED DIMENSION OF VARIOUS PARAMETERS OF PROPOSED RADIATOR

Symbol	Dimension [mm]	Symbol	Dimension [mm]
Ls	80.0	Lm	102.0
Ws	40.0	Wm	60.0
H1	8.0	L1	9.0
H2	1.6	L2	2.0
L3	9.0	Lp	20.0
Lf	12.0	Wp	20.0
Wf	2.7	G	0.8

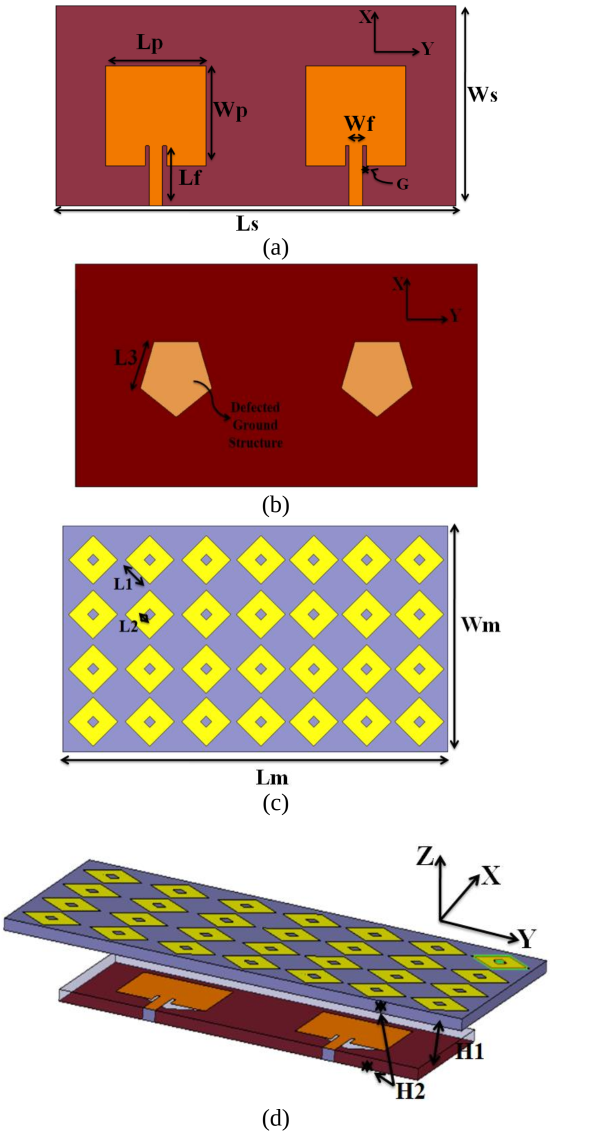

Fig. 1. Proposed antenna design: (a) top view, (b) bottom view, (c) proposed metasurface, and (d) 3D view.

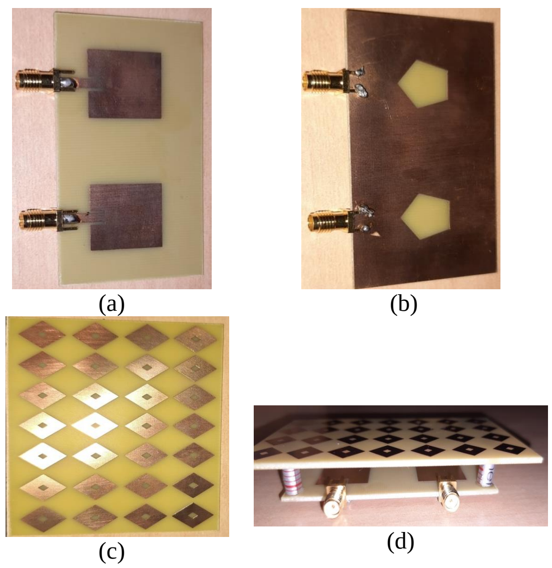

Fig. 2. Fabricated pictures of proposed antenna: (a) top view, (b) bottom view, (c) metasurface, and (d) 3D view.

III. Antenna Analysis

In this section, the proposed radiator has been analyzed with the assistance of HFSS EM simulator. The complete analysis of proposed antenna is divided in two parts: (i) single port analysis; and (ii) dual port analysis.

i. Single Port Analysis

Fig. 3 shows the reflection coefficient variation with square patch antenna with simple microstrip line as well as inset feed. From Fig. 3, it can be observed that inset feed improves the impedance matching level in the complete frequency range [9]. Two resonant peaks are also occurs at 12.3 GHz and 13.4 GHz. Fig. 4 shows the E-field variation at 12.3 GHz and 13.4 GHz. From Fig. 4, it is confirmed that the resonant peaks at 12.3 GHz and 13.4 GHz are due to TM_{21} and TM_{22} mode respectively [10]. Fig. 5 presents the $|S_{11}|$ variation with and without pentagon shaped defected ground structure (DGS). From Fig. 5, it is observed that by applying the DGS, the overall Q-factor of radiator decreases which in turn improves the bandwidth [11]. Resonant peaks are also shifted to higher frequency with increases in the size of DGS. It is due to reduction in the effective permittivity of the radiator.

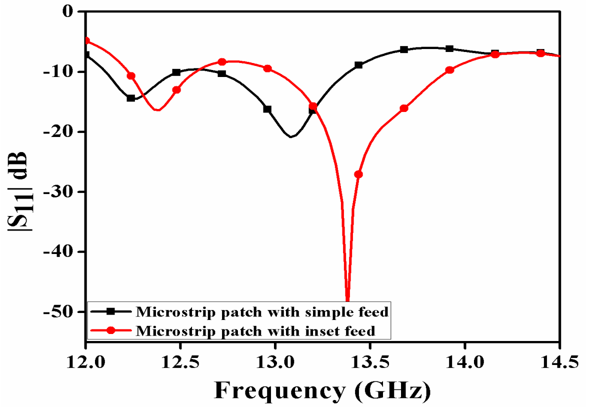

Fig. 3. $|S_{11}|$ variation for single port microstrip antenna with simple microstrip line feed and inset feed.

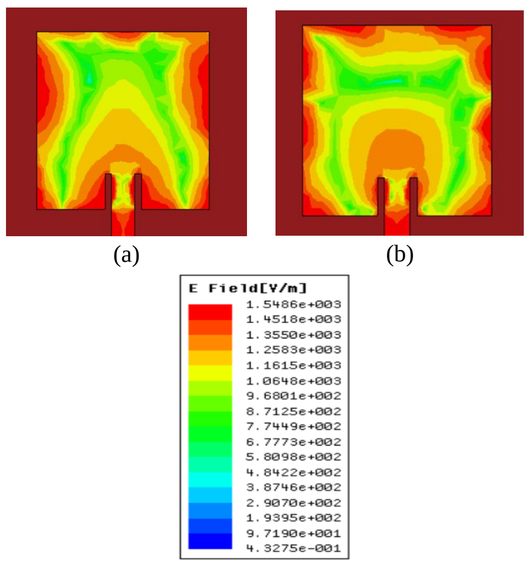

Fig. 4. E-field variation on radiator: (a) 12.3 GHz and (b) 13.4 GHz.

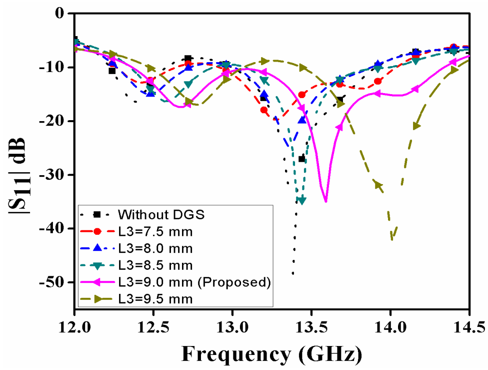

Fig. 5. $|S_{11}|$ variation for single port microstrip antenna with DGS and without DGS.

ii. Dual Port Analysis

Fig. 6 shows the S-parameter variation with single port and dual port. From Fig. 6, it can be said that conversion of single port in to dual port without any modification, relatively same impedance bandwidth is achieved. Isolation level is also more than 25 dB within the operating band. Now, a metasurface, which is made up of a periodic arrangement of ring shaped rhombus unit cell. It is suspended over the dual port printed radiator. Fig. 7 shows the permeability and permittivity variation of unit cell over the operating frequency range. From Fig. 7, it can be said the permittivity is negative over the operating band, while permeability is positive. Therefore, it behaves as single negative group (SNG) metamaterial. When such type of metasurface is suspended over the radiator, it creates the EM wave evanescent. By doing so, mutual coupling reduces between antenna ports [12].

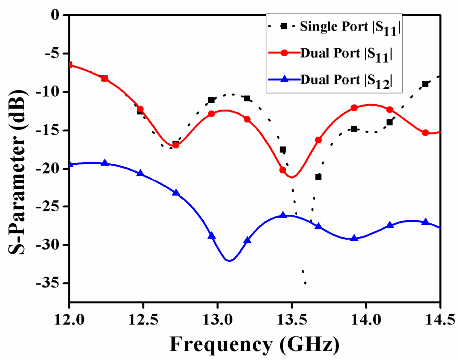

Fig. 6. S-parameter variation with single and dual port radiator.

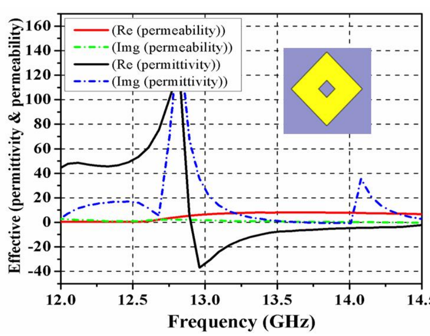

Fig. 7. Effective permittivity and permeability of unit cell over the complete frequency range.

Fig. 8 presents the S-parameter variation of dual port antenna with and without metasurface. From Fig. 8, it is observed that isolation level between the ports has been improved to more than 35 dB, after applying the metasurface. The same metasurface is also used for conversion of linear polarized wave to circular polarized wave. Fig. 9 presents the E-field arrangement over the metasurface. Upward and adjacent gaps between the cells of metasurface classify the linear polarized waves into horizontal and vertical waves with different angles i.e. 0°, 90°, 180°, 270°. It satisfies the condition of circular polarization i.e. degenerated orthogonal mode creation with equal amplitude and 90° shift between these orthogonal modes [13].

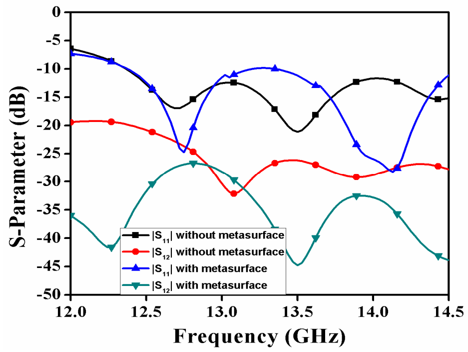

Fig.8. S-parameter variation of dual port antenna with and without metasurface.

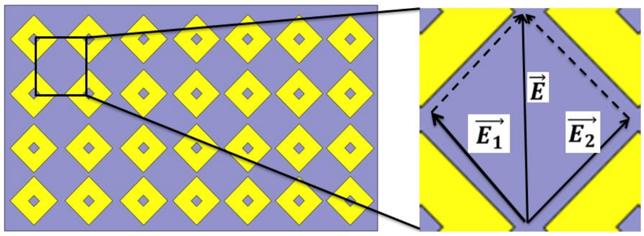

Fig. 9. Vector E-field alignment on metasurface for CP waves creation.

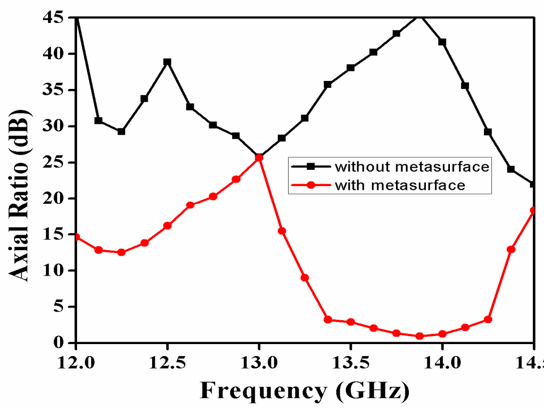

Fig. 10. Axial ratio variation with and without metasurface.

Fig. 10 shows the axial ratio variation with and without metasurface. From Fig. 10, it is observed that CP waves are created with the help of metasurface and supports CP waves from 13.3 GHz to 13.87 GHz. Fig. 11 shows the axial ratio variation with change in height of metasurface with respect to the radiating surface. From Fig.11, it is confirmed that the optimized 3-dB AR bandwidth is achieved at the height of 8.0 mm.

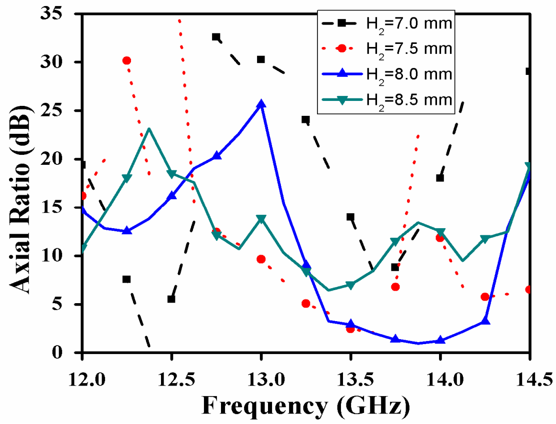

Fig. 11. Axial ratio variation with change in height of metasurface w.r.t radiating surface.

IV. EXPERIMENTAL OUTCOME AND DIVERSITY PARAMETER

In this section, optimized simulated outcomes are finally compared with experimental results, which are obtained by verification of prototype shown in Fig. 2. S-parameter of proposed antenna is measured with of E8363C Keysight based PNA. Fig. 12 presents the comparison of simulated and measured S-parameter variation. From Fig. 12, it is confirmed that the proposed antenna works from 12.2 GHz to 14.2 GHz with isolation level more than 38 dB. There is good agreement between measured and simulated S-parameter. Some variation is observed due to different fabrication tolerances such as soldering of connector over the substrate. Fig. 13 presents the measured and simulated axial ratio variation of proposed radiator. It is measured with dual linear pattern measurement [13]. During measurement, one port is excited while other one is terminated with match load. From Fig. 13, it can be said that the proposed antenna supports CP waves from 13.2 GHz to 13.9 GHz. There is also a good agreement between measured and simulated AR. Some error occurs may be due misalignment with reference antenna.

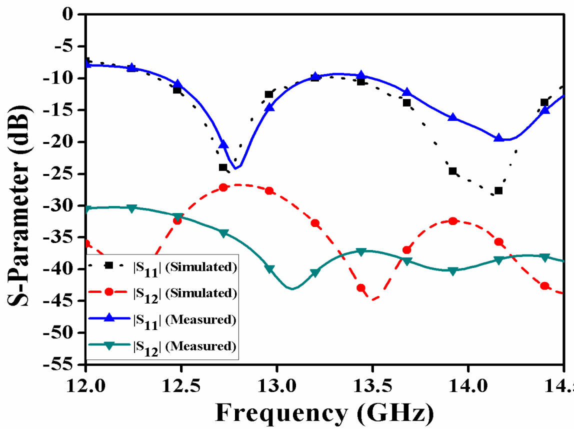

Fig. 12. Measured and simulated S-parameter of proposed dual port microstrip antenna.

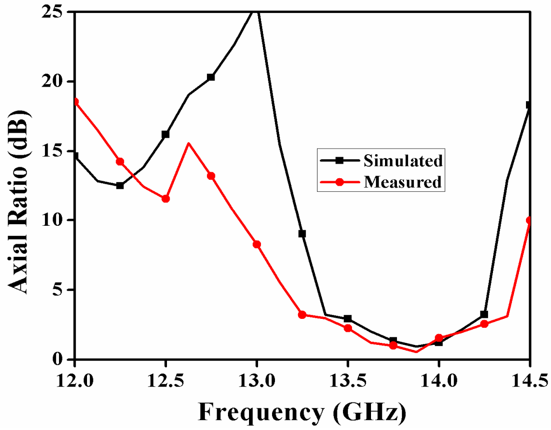

Fig. 13. Measured and simulated axial ratio of proposed dual port microstrip antenna.

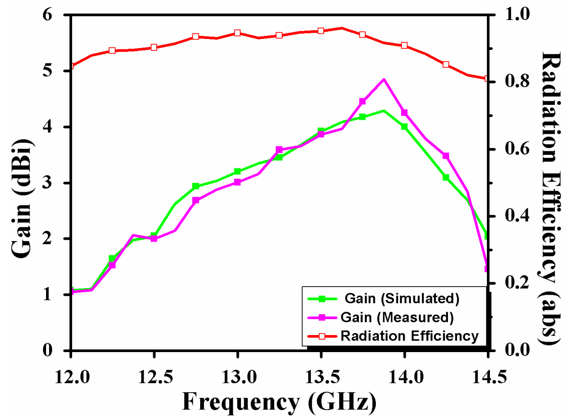

Fig. 14. Gain (measured and simulated) and radiation efficiency (simulated) of proposed dual port microstrip antenna.

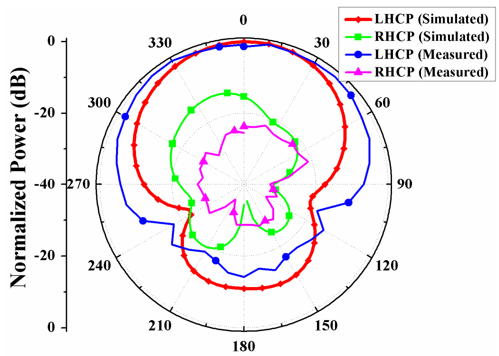

(a)

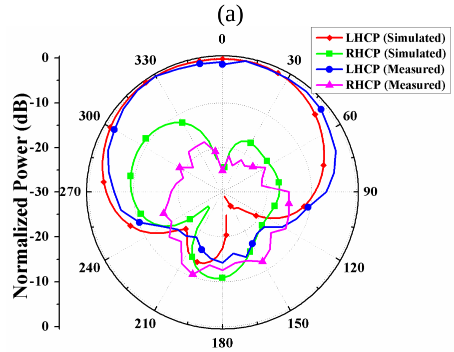

(b)

Fig. 15. LHCP and RHCP (measured/simulated) of proposed radiator in XZ plane at 13.8 GHz: (a) port-1 and (b) port-2.

Fig. 14 presents the gain (measured and simulated) and radiation efficiency (simulated) curve of proposed antenna. Gain is measured with two antenna method [13]. From Fig. 14, it is observed that maximum gain is around 4.9 dBi within the operating band, while efficiency is around 90% within the operating band. Fig. 15 shows the LHCP and RHCP radiation pattern of proposed antenna in XZ plane at 13.8 GHz with port-1 and port-2 respectively. Radiation pattern is measured with single port, while other port is terminated with match load [14]. From Fig. 15, it is confirmed that broadsided radiation pattern is obtained with both the antenna ports. The proposed antenna behaves as left handed circularly polarized with both the ports because LHCP is more dominant in comparison to RHCP. Table 2 lists the performance of proposed MIMO antenna with other existing radiator in terms of axial ratio bandwidth, impedance bandwidth, isolation level and gain. From Table 2, it can be concluded that the proposed radiator has better overall performance in comparison to other one.

TABLE 2
PERFORMANCE COMPARISON OF PROPOSED ANTENNA WITH OTHER EXISTING PRINTED ANTENNAS

Antennas	Impedance bandwidth	Axial ratio bandwidth	Isolation level	Gain [dBi]
Rectangular microstrip with superstrate [3]	40 MHz	NA	>25 dB	4.5
Dielectric loaded microstrip antenna [4]	690 MHz	NA	>30 dB	6.0
FSS loaded microstrip antenna [5]	3.5 GHz	NA	>35 dB	7.5
Z-shaped printed antenna [6]	4.01 GHz	1.5 GHz	>20 dB	2.5
Diagonally perturbed printed antenna [7]	450 MHz	92 MHz	>30 dB	5.34
Reflector loaded printed monopole antenna [8]	1.1 GHz	1.1 GHz	>20 dB	5.8
Proposed antenna	**2.2 GHz**	**700 MHz**	**>38 dB**	**4.9**

In case of MIMO antenna, it is important to evaluate the diversity parameters such as envelop correlation coefficient (ECC) and diversity gain (DG). ECC tells us about the correlation of antenna ports, which should be minimum for efficient MIMO antenna. Diversity gain (DG) tells about the overall gain of antenna in the fading environment. It is measured by using following formula [1]:

$$\mathrm{ECC} = \frac{|S_{11}^{*}S_{12} + S_{21}^{*}S_{22}|^2}{\left(\left(1-(|S_{11}|^2+|S_{21}|^2)\right)\left(1-(|S_{22}|^2+|S_{12}|^2)\right)\right)} \quad (1)$$

$$\mathrm{DG} = 10\sqrt{(1-|\rho|^2)} \quad (2)$$

Fig. 16 presents the ECC and DG variation of proposed antenna. From Fig. 16, it is confirmed that the value of ECC is quite below to 0.3, while the value of DG is approx. 10 dB within the operating band. So, it can be said that the proposed radiator is an efficient MIMO antenna.

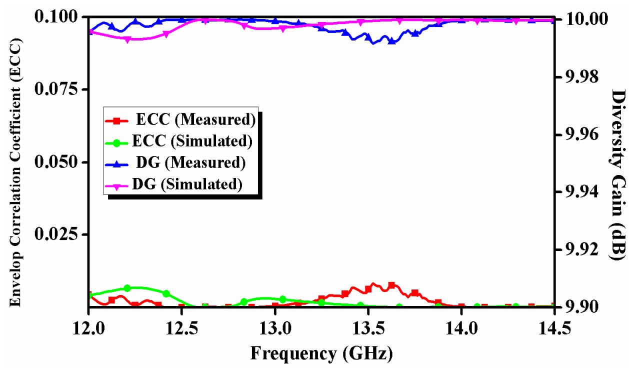

Fig. 16 ECC and DG variation of proposed MIMO microstrip antenna.

V. CONCLUSION

In this article, a dual port microstrip antenna is designed and analyzed. A metasurface is suspended over the radiator for solving the two purposes: (a) acts as LP to CP convertor within the operating band and provides the CP waves from 13.2 GHz to 13.9 GHz; and (b) for improving the isolation level (more than 38 dB) between the antenna ports. The proposed radiator also contains the DGS for reducing the Q-factor value and enhances the bandwidth. The proposed antenna works from 12.2 GHz to 14.2 GHz. Good diversity parameter and far-field parameters of proposed antenna makes it suitable for Ku band satellite application.

REFERENCES

[1] M.S. Sharawi, *Printed MIMO Antenna Engineering*, Artech House (Boston, London), 2014.

[2] C.A. Balanis, *Antenna Theory: Analysis and Design*, John Wiley and Sons, USA, 2005.

[3] Z. Niu, H. Zhang, Q. Chen and T. Zhong, "Isolation Enhancement in Closely Coupled Dual-Band MIMO Patch Antennas", *IEEE Antennas and Wireless Propagation Letters*, vol. 18, no. 8, pp. 1686-1690, August 2019, doi: 10.1109/LAWP.2019.2928230.

[4] M. Li, M. Y. Jamal, L. Jiang and K. L. Yeung, "Isolation Enhancement for MIMO Patch Antennas Sharing a Common Thick Substrate: Using a Dielectric Block to Control Space-Wave Coupling to Cancel Surface-Wave Coupling", *IEEE Transactions on Antennas and Propagation*, vol. 69, no. 4, pp. 1853-1863, April 2021, doi: 10.1109/TAP.2020.3026897.

[5] Md. M. Hasan, M.T. Islam, Md Samsuzzaman, M.H. Baharuddin, M.S. Soliman, A. Alzamil, I. I.M. Abu Sulayman and Md. S. Islam, "Gain and Isolation Enhancement of a Wideband MIMO Antenna Using Metasurface for 5G Sub

6GHz Communication Systems", *Scientific Reports*, vol. 12, Article number 9433, 2022, pp. 1-17, doi: 10.1038/s41598-022-13522-5.

[6] R.N. Tiwari, P.Singh, B.K. Kanaujia and P. Kumar, "Compact Circularly Polarized MIMO Printed Antenna with Novel Ground Structure for Wideband Applications", *International Journal of RF and Computer Aided Engineering*, vol. 31, no. 8, August 2021, e22737, doi: 10.1002/mmce.22737.

[7] L. Malviya, R.K. Panigrahi, and M.V. Kartikeyan, "Circularly Polarized 2×2 MIMO Antenna for WLAN Applications", *Progress In Electromagnetic Research C*, vol. 66, 2016, pp. 97-107, doi: 10.2528/PIERC16051905.

[8] U. Ullah, I.B. Mabrouk and S. Koziel, "Enhanced-Performance Circularly Polarized MIMO Antenna with Polarization/Pattern Diversity", *IEEE Access*, vol. 8, pp. 11887-11895, 2020, doi: 10.1109/ACCESS.2020.2966052.

[9] M. Ramesh and K.B. Yip, "Design Formula for Inset Fed MicrostripPatch Antenna", *Journal of Microwaves and Optoelectronics*, vol. 3, no. 3, 2003, pp. 5-10.

[10] S. Naik and M. Pour, "A Miniaturized TM21 Mode Circular Microstrip Patch Antenna", *Progress In Electromagnetics Research Letters*, vol. 83, pp. 45-50, 2019, doi:10.2528/PIERL19020303.

[11] T. Sarkar, A. Ghosh, L. L. K. Singh, S. Chattopadhyay and C. -Y. -D. Sim, "DGS-Integrated Air-Loaded Wideband Microstrip Antenna for X- and Ku-Band", *IEEE Antennas and Wireless Propagation Letters*, vol. 19, no. 1, pp. 114-118, Jan. 2020, doi: 10.1109/LAWP.2019.2955111.

[12] Z. Wang, L. Zhao, Y. Cai, S. Zheng, and Y. Yin, "A Meta-Surface Antenna Array Decoupling (MAAD) Method for Mutual Coupling Reduction in a MIMO Antenna System", *Scientific Reports*, vol. 8, Article number: 3152, 2018, pp. 1ï 9, doi: 10.1038/s41598-018-21619-z.

[13] W.L. Stutzman and G.A. Thiele, *Antenna Theory and Design*, JohnWiley& Sons, Hoboken, NJ, 2013.

[14] G. Das, A. Sharma and R.K. Gangwar, "Dielectric Resonator Based Circularly Polarized MIMO Antenna with Polarization Diversity", *Microwave and Optical Technology Letters*, vol. 60, no. 3, March 2018, pp. 685-693, doi: 10.1002/mop.31033.